Structural evolution of inner voids and interface of electrode-solid electrolyte of all-solid-state lithium-ion-batteries by annealing

Yamamoto, Y.[1], Iriyama, Y.[2] and Muto, S.[1]

[1] High Voltage Electron Microscope Laboratory, Nagoya University, Japan, [2] Department of Materials Design Innovation Engineering, Nagoya University, Japan

All-Solid-State Lithium-Ion-Battery (ASS-LIB) has attracted attention as an alternative rechargeable battery. An aerosol deposition (AD) method [1] was applied to fabricate an ASS-LIB composite thin film composed of a lithium (Li) transition metal-oxide electrode and a Li^+ conductive oxide-based solid electrolyte with their internal densities improved [2]. However, several-tenths volume % of voids exist inside the composite electrode on a model substrate formed by AD [3], the volume of which was reported to decrease by annealing [4]. In this study, we investigated the structure of the annealed/non-annealed composite electrodes on lithium-lanthanum-zirconate (LLZ) which has recently attracted attention as a solid electrolyte part of ASS-LIB using the void analysis [3] and the interfacial structure analysis.

A composite electrode composed of $LiCoO_2$ (LCO) electrode and Li^+ conductive oxide-based solid electrolytes, Li-Al-Ti-P-O glass ceramics (LATP) manufactured by Ohara Inc. [5], were prepared on the LLZ substrate by AD, then annealed at 400℃ for 1h in dry-air. A 3D structural data-cube was obtained by automatic alternating operations of SEM observation and FIB cross-sectioning, using an orthogonal FIB/SEM system (MI4000L, HITACHI), followed by image-processing for the void analysis (alignment of SEM images, volume rendering, applying filters and union operation) using the software, Avizo fire (Thermo Fisher Scientific). In addition, a STEM-EELS data-cube was also obtained by an aberration-corrected STEM (JEM-ARM200F, JEOL), operated at 200kV, using a liquid nitrogen cooling holder. The STEM-EELS data-cube were analyzed by a non-negative matrix factorization (NMF) technique to isolate and visualize the different chemical components involved [6].

Figures 1(a) and (b) show the 3D void distributions in the composite before and after the heat treatment, respectively. The void volume ratios were estimated to be 0.50% and 0.15% for (a) and (b), respectively. Figure 2 summarizes the STEM-EELS results for a pristine LATP particle ($LiTi_2(PO_4)_3$) [5]. Figure 2(a) shows the HAADF-STEM image of the small region-of-interest, (b) the projected lithium content normalized by the sample thickness, and (c) and (d) the spatial distributions of different chemical components of Ti and O extracted by NMF with the corresponding sets of the Ti-$L_{2,3}$ and O-K spectra shown in (e) and (f), respectively. The onset of the Ti-$L_{2,3}$ and O K spectra in (e) is sifted to the lower energy side compared to that in (f). In addition, the relative intensity of the O K with respect to the Ti-$L_{2,3}$ in (e) is significantly smaller than that in (f), which implies Li-rich, Ti-reduced and O-poor outside the LATP particle.

Figures 3 and 4 illustrate the STEM-EELS analysis results of the interface between LCO and LATP in the composite before and after the heat treatment, respectively. The Li-rich layer is formed on the LATP side adjoining the interface in Fig. 3, due to the surface structure of the pristine LATP particle. In the annealed composite, on the other hand, no Ti-reduced region partially connected to LCO is observed. In conclusion, the annealing the composite fabricated by AD results in the reduction of the void volume over the entire region and formation of novel interface structure.

[1] Akedo J. J. Am. Ceram. Soc. 89 (2006) 1834-1839
[2] Kato T. et al., J. Power Sour. 303 (2016) 65-72
[3] Yamamoto Y., Iriyama Y., Muto S. Microscopy 65 (2016) 191-198
[4] Yamamoto Y., Iriyama Y., Muto S. M&M 23 (2017) 314-315
[5] Jie F. J. Am. Ceram. Soc. 80 (1997) 1901-1903
[6] Muto S., Tatsumi K. Microscopy 66 (2017) 39-49

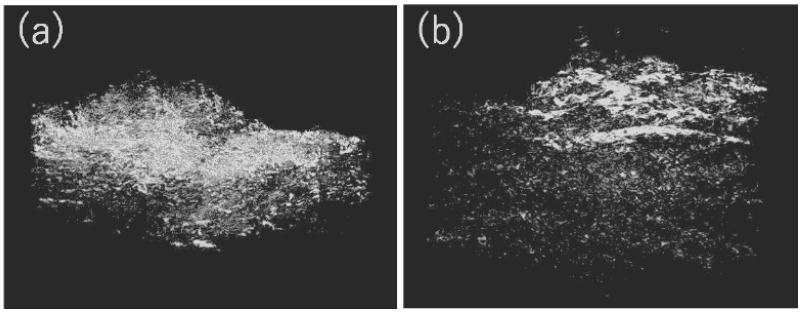

Figure 1 3D void configurations of non-heat-treated (a) and annealed composite electrode (b), respectively.

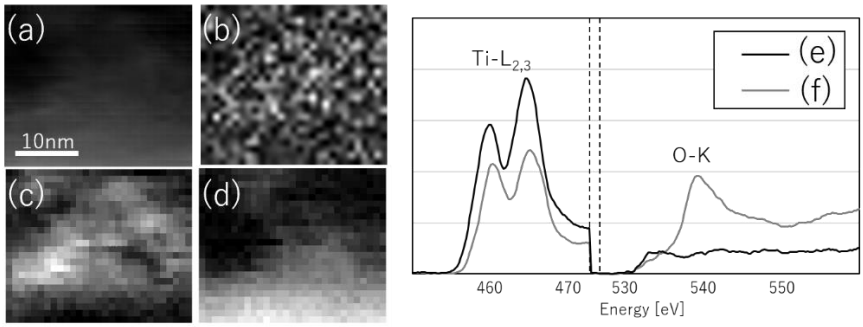

Figure 2 NMF analysis results of pristine LATP particle. (a) HAADF-STEM image. (b) Lithium content map. (c), (d) Spatial distributions of two chemical components separated by NMF. (e), (f) EELS corresponding to (c) and (d), respectively. Ti is reduced in (c), while not reduced in (d).

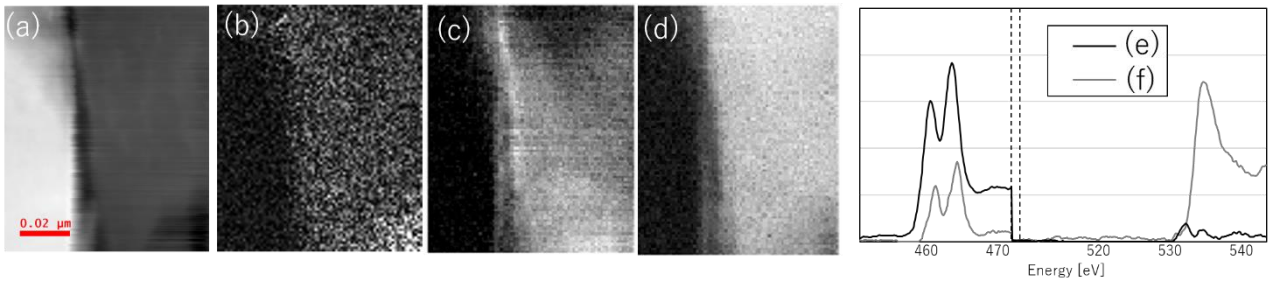

Figure 3 NMF analysis results of the interface between LATP and LCO of non-heat-treated composite. (a) HAADF-STEM image. (b) Lithium content map. (c), (d) Spatial distributions of different chemical components separated by NMF. (e), (f) EELS corresponding to (c) and (d), respectively. Ti is reduced in (c) while not reduced in (d).

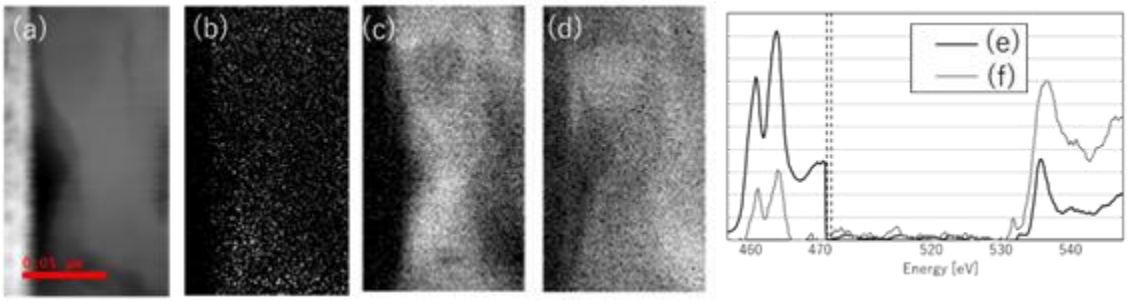

Figure 4 NMF analysis results of the interface between LATP and LCO of annealed composite. (a) HAADF-STEM image. (b) Lithium content map. (c), (d) Spatial distributions of different chemical components separated by NMF. (e), (f) EELS corresponding to (c) and (d), respectively. Ti is reduced in (c) while not reduced in (d).